Diffusion-limited exciton-exciton annihilation in single-walled carbon nanotubes: A time-dependent analysis

Ajit Srivastava* and Junichiro Kono
Department of Electrical and Computer Engineering, Rice University, Houston, Texas 77005, USA
(Received 31 October 2008; revised manuscript received 2 April 2009; published 8 May 2009)

To provide physical insight into the recently observed photoluminescence saturation behavior in single-walled carbon nanotubes implying the existence of an upper limit of exciton densities, we have performed a time-dependent theoretical study of diffusion-limited exciton-exciton annihilation in the general context of reaction-diffusion processes, for which exact treatments exist. By including the radiative recombination decay as a Poissonian process in the exactly solvable problem of one-dimensional diffusion-driven two-particle annihilation, we were able to correctly model the dynamics of excitons as a function of time with different initial densities, which in turn allowed us to reproduce the experimentally observed photoluminescence saturation behavior at high exciton densities. We also performed Monte Carlo simulations of the purely stochastic, Brownian diffusive motion of one-dimensional excitons, which validated our analytical results. Finally, by considering the diameter, chirality, and temperature dependence of this diffusion-limited exciton-exciton annihilation, we point out that high exciton densities in single-walled carbon nanotubes may be achieved at low temperature in an external magnetic field.

DOI: 10.1103/PhysRevB.79.205407 PACS number(s): 78.67.Ch, 71.35.−y, 78.55.−m

I. INTRODUCTION

Excitons in single-walled carbon nanotubes (SWNTs) are stable quasiparticles with large binding energies and significantly influence their interband optical properties.[1] However, they have been reported to be rather efficiently eliminated at high densities through the exciton-exciton annihilation (EEA) process,[2] although their emission and absorption energies remain stable even at high densities.[3] Recently, the intensity of photoluminescence (PL) from SWNTs was found to saturate at high pump fluence, implying the existence of an upper limit in the density of excitons, which was estimated to be an order of magnitude smaller than the expected Mott density[4] (the density at which the interexciton distance becomes comparable to the Bohr radius[5]). The existence of such an upper limit, which poses a significant hindrance in the observation of lasing, a Mott transition, or excitonic Bose-Einstein condensation in SWNTs, was attributed to efficient EEA facilitated by the diffusive motion of excitons in agreement with previous claims.[6–8]

The dynamics of diffusion-limited EEA can be analyzed in the general context of reaction-diffusion processes, which have been extensively studied by physicists, chemists, biologists, and ecologists and serve as simple models for studying a variety of nonequilibrium problems.[9–13] Moreover, it has been shown that such simple diffusion-driven reactions exhibit interesting nonequilibrium phase transitions and universality classes,[14] with connections to many-body theory.[15,16] In such models, particles, or "agents," of one or more species execute random walk in d dimensions (where d could also be fractional in the case of fractal geometry) and undergo reactions upon collisions, leading to changes in their population often accompanied by an appearance and disappearance of various phases. Such systems often exhibit rich phase diagrams that can be fully studied with numerical simulations even when analytical solutions are not available. For example, a widely studied reaction is the two-particle annihilation given by $A+A\rightarrow 0$, where the interaction is assumed to be of the "hard-core" type, leading to the mutual destruction of two particles upon collision.[10] Starting with an initial population N_0, one can analyze the ensemble averaged population N_t at a given time t. Clearly, this is a nonequilibrium many-particle process that is driven by noise, and its only steady state is achieved when the population vanishes.

An interesting feature of diffusion-driven reactions is the presence of spatio-temporal fluctuations in such processes that cannot be ignored especially at lower dimensions and lead to the breakdown of mean-field type assumptions. For example, diffusion-driven two-particle annihilation can be written in differential form as follows:[10]

$$\partial_t\langle n(x,t)\rangle = D\nabla^2\langle n(x,t)\rangle - \langle n^2(x,t)\rangle, \tag{1}$$

where $\langle . \rangle$ stands for an ensemble average. The first term on the right denotes the diffusion process, while the second term is for two-particle annihilation and thus has quadratic dependence. Note that the annihilation term has an average of $n^2(x,t)$ whereas mean-field theory will simplify this to $\langle n(x,t)\rangle^2$, thus neglecting fluctuations of the form $\langle n^2(x,t)\rangle - \langle n(x,t)\rangle^2$. In one dimension, the population asymptotically decays as $t^{-1/2}$ power law whereas the mean-field theory, which ignores fluctuations, predicts a faster decay of t^{-1}. This discrepancy originates from the fact that d-dimensional diffusion with $d \leq 2$ is *recurrent* and the particles return to their previous position with high probability.[17] Hence, the reaction is slowed down leading to a smaller exponent in the power-law decay. Indeed, the mean-field result is recovered in three dimensions, which is above the critical dimension $d_c=2$ for this problem.[18] Thus, an exact treatment of the dynamics of even such a simple process requires the inclusion of correlations.

II. MODEL DETAILS

In this paper, motivated by the recent experimental observation of an upper limit in the density of excitons,[4] we un-

dertake a time-dependent study of a one-dimensional diffusion-limited EEA process in the presence of radiative decay. In our model, we assume that an initial population of N_0 pairs of excitons is created along the nanotube of length L under the excitation of an ultrashort laser pulse of sufficient photon energy. We further assume that the laser excitation spot is larger than L, leading to the creation of excitons that are randomly distributed along the nanotube. After the laser pulse is gone, the excitons start diffusive motion along the nanotube, possibly arising from random collisions with phonons.[8] We treat excitons as point particles that execute one-dimensional random walk along the length of the nanotube and undergo annihilation upon crossing each other. In reality, excitons have a finite spatial extent given by their Bohr radius, a_B, which is expected to be $\sim 1-1.5$ nm for nanotubes with diameter ~ 1 nm.[19] Thus, our treatment of excitons as point-particles is valid when the interexciton distance is greater than a_B, or in other words, when the excitonic density is below the Mott density. In addition to the decay via EEA, the exciton population decays radiatively with a lifetime τ_r.

We consider the following two coupled and competing reaction-diffusion processes in one dimension (1D) to model the dynamics of excitons in nanotubes at various densities,

$$A + A \rightarrow kA \quad (k = 0,1), \tag{2a}$$

$$A \xrightarrow{\gamma_r} B, \tag{2b}$$

where A represents excitons and B photons. The first equation represents exciton-exciton annihilation, which is either complete ($k=0$) or partial ($k=1$), while the second reaction is just the radiative decay of excitons with radiative lifetime $\tau_r = 1/\gamma_r$. It is noteworthy that only the first reaction is diffusion-driven whereas as the radiative decay takes place independently. In this sense, there are two temporal noise terms—the annihilation reaction is driven by diffusive noise, which we assume to be of the Gaussian form, whereas the radiative decay is governed by a Poissonian noise and, hence, is a pure jump process. We do not include any other nonradiative processes in our model but it is straightforward to include them by simply replacing τ_r with an effective lifetime τ as long as they also follow Poissonian statistics. The rate of creation of photons (B) would then decrease by a factor equal to the branching ratio of the radiative and the nonradiative processes. We consider a simple diffusion process in which the diffusion constant D is independent of the spatial and temporal coordinates. Furthermore, the length of the nanotube L is assumed to be much larger than the excitonic dimension.

We are interested in determining the population of both species as a function of time. The population of species B, or photons, is proportional to the PL intensity measured experimentally. In particular, we wish to know the fraction of population which decays radiatively and how this fraction changes as the initial population is increased. As one can imagine, upon increasing the initial density of excitons in the 1D nanotube the annihilation reaction becomes more efficient whereas the radiative decay rate can be safely assumed to be independent of the density. As we show later, this leads to saturation of the PL intensity as the initial population density is increased, which is consistent with the experimental observations.[4]

In Sec. IV, we compare our results to that of the recent experimental observation of PL saturation[4] and find excellent quantitative agreement. In our generic model, which applies to any one-dimensional system, the only physical parameters are the interexciton distance $d_0 = L/2N_0$, the diffusion constant D, and the radiative lifetime τ_r. However, to interpret our results in terms of carbon nanotube parameters such as diameter, chirality, and other excitonic energy scales, we need to consider the dependence of our model parameters on them. This is done in Sec. V along with a discussion on the effect of temperature on the EEA process. In Sec. III, we obtain analytical results for the populations of excitons and photons as a function of time using the first-passage time distribution of Brownian motion and compare them to numerical simulations done using the Monte Carlo technique.

III. SOLUTION USING FIRST-PASSAGE DISTRIBUTION

The case of two-particle annihilation without the radiative decay has been extensively studied, and exact results for the population as a function of time are known.[20–23] In the context of carbon nanotubes, there have been a few studies on carrier and exciton dynamics in the presence of Auger ionization and radiative decay, involving solutions of master equation for the time-dependent occupation probability.[24,25] Here we use the first-passage time distribution of Brownian motion to first study the annihilation reaction without decay. We recover the exact analytical results for this case before proceeding to include the radiative decay term. We begin by deriving the exact result for a single pair, or the "independent pairs" case, and use it to obtain an approximate solution for the many-particle, or the "correlated" case. Monte Carlo simulations are performed to check the validity of our results. This purely stochastic method employing the first-passage time distribution is a simple and natural way to study the annihilation reaction as the collisions which drive the reactions must obey such distributions.

A. Annihilation without decay; $k=0$

Consider N_0 pairs of species A randomly arranged on a line of length L and executing Brownian diffusion with diffusion constant D. Let us first consider just the two-particle annihilation process without the decay as in Eq. (2a) with $k=0$. Let $n_A(t)$ denote the average fraction of initial population which is still "alive" at time t. We keep the discussion in this section as general as possible without explicitly identifying species A or B unless absolutely required.

In 1D, only the nearest neighbors at any given time can undergo annihilation due to restrictions placed by lower dimensionality. This prompts us to first consider the case for a single pair of particles and generalize the result to the many-particle case. As this is equivalent to different pairs annihilating independently of each other, we refer to it as the "in-

dependent pair" case. Let d_0 be the initial distance between the pair and $P(d_0,t)$ denote the survival probability of this pair at time t. To calculate $P(d_0,t)$, we need to find the probability that a pair with initial distance d_0 does not undergo collision until time t. As both particles are executing independent Brownian motion, their relative motion is also Brownian with diffusion constant $2D$ which starts at d_0. Thus, we need to find the probability that a Brownian motion starting at d_0 does not reach zero until time t. This can be readily found from the first-passage time distribution of a Brownian motion as[26]

$$P(d_0,t) = \mathrm{erf}\left(\frac{d_0}{2\sqrt{Dt}}\right), \tag{3}$$

where erf(.) is the error function. For the independent pair case, the fraction of population that is alive at time t, $n_A(t)$, reads

$$n_A(t) = \sum_{i=1}^{N_0} \mathrm{erf}\left(\frac{d_{0,2i}}{2\sqrt{Dt}}\right) = \sum_{i=1}^{N_0} \mathrm{erf}\left(\frac{d_{0,2i-1}}{2\sqrt{Dt}}\right), \tag{4}$$

where the distance between the particles of the ith pair is $d_{0,i}$ at time $t=0$. We have imposed a periodic boundary condition making the line into a ring without any loss of generality. As N_0 tends to infinity, the above sum can be expressed as an integral over the distribution of $d_{0,i}$s. We restrict ourselves to the case when the particles are randomly arranged on the line at $t=0$. Thus, $d_{0,i}$s which are the distances between pairs can be thought of as the "waiting times" for a Poisson process and have an exponential distribution spatially along the nanotube with mean $d_0=L/2N_0$.

For the many-particle case we realize that there are twice as many ways for a pair to annihilate as for the independent case due to the presence of two nearest neighbors for each particle, and hence, the mean distance for the correlated case is just a half of the independent case in the large N_0 limit. For this limit, the exact result can be obtained as

$$n_A(t) = \int_0^\infty dx\beta \exp(-\beta x)\mathrm{erf}\left(\frac{x}{2\sqrt{Dt}}\right)$$
$$= \exp(\beta^2 Dt)\mathrm{erfc}(\sqrt{\beta^2 Dt}), \tag{5}$$

which is the result of Torney *et al.*[20] with $\beta=4N_0/L$. In the asymptotic limit, Eq. (5) yields a power-law decay of $t^{-1/2}$ as mentioned earlier.

At long times the initial correlations between the particles are completely wiped out, and this power-law decay is expected, irrespective of the initial distribution of particles. Such a power-law behavior has been recently observed in time-resolved transient absorption measurements on SWNTs.[7]

B. Annihilation with decay; $k=0$: Independent pair case

Next, we include radiative decay of Eq. (2b) in our model and compute the population fraction of species A and B as a function of time. As before, we first derive the exact result for the case of a single pair and use it as a kernel to express the result for independent pairs uniformly distributed along the tube. For a single pair separated by a distance d_0 at $t=0$, the surviving population fraction at t can be simply written as

$$n_A(t) = \frac{1}{2}\sum np(n,t) \quad (n=0,1,2), \tag{6}$$

where $p(n,t)$ denotes the probability of n surviving particles at time t, which remains to be calculated. Let us compute $p(2,t)$, which is the probability that both particles comprising the pair are alive at time t. Such a case is possible *only* if neither particle undergoes radiative decay or collision until time t. As the radiative decay of particles occurs independently of one another and also of the diffusion-driven collision, we can simply multiply the individual probabilities to get

$$p(2,t) = \exp(-2\gamma_r t)\mathrm{erf}\left(\frac{d_0}{2\sqrt{Dt}}\right). \tag{7}$$

Recall that radiative decay is a Poisson process with parameter γ_r and the probability of it not happening until time t is $\exp(-\gamma_r t)$. To compute $p(1,t)$, which is the probability that *exactly* one particle out of the pair survives, we realize that such a scenario is possible *only* if there is exactly one radiative decay in the time interval $[0,t]$, say at $t=\tau$, and no collision *before* τ. As in the interval (τ,t) collisions cannot take place due to an insufficient number of particles for the reaction, we only include the probability of collision not taking place before τ. The probability that either of the particles decay in an infinitesimal interval $d\tau$ about τ is $2\gamma_r d\tau$. As before, we can multiply the probabilities for each subevent due to mutual independence. Thus,

$$p(1,t) = \int_0^t \exp(-2\gamma_r\tau)\mathrm{erf}\left(\frac{d_0}{2\sqrt{D\tau}}\right)$$
$$\times(2\gamma_r d\tau)\exp[-2\gamma_r(t-\tau)]. \tag{8}$$

From Eqs. (6)–(8), $n_A(t)$ for a single pair can be obtained. As before, for the case of N_0 independent pairs, we average $n_A(t)$ over an exponential distribution with mean $d_0=L/2N_0$. After some straightforward but tedious algebra we obtain

$$n_A(t) = \frac{\exp(-\gamma_r t)}{1-\nu}\left[\exp\left(\frac{1-\nu}{\nu}\gamma_r t\right)\mathrm{erfc}(\sqrt{\gamma_r t/\nu})\right.$$
$$\left. + \sqrt{\nu}\,\mathrm{erf}(\sqrt{\gamma_r t}) - \nu\right], \tag{9}$$

where we have introduced a dimensionless parameter $\nu = \tau_D/\tau_r$ with τ_D being the "diffusional time" d_0^2/D. We emphasize that this is an *exact* result for the case of independently colliding pairs that also undergo radiative decay. The above equation is valid only when $\nu<1$, or, in other words, when radiative decay is slower. In the limit of extremely dilute initial population density, no annihilation can take place, and only radiative decay occurs. $n_A(t)$ would be simply $\exp(-\gamma_r t)$ in that case. In the opposite limit when radiative decay rate γ_r vanishes, Eq. (9) indeed recovers the result of Eq. (5), as expected.

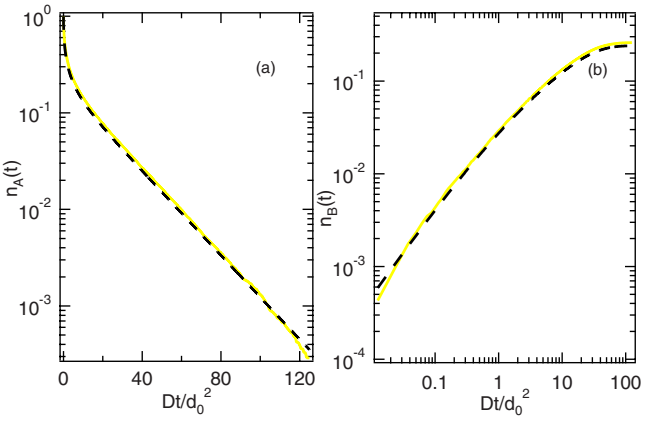

FIG. 1. (Color online) Comparison of Monte Carlo simulations (solid line) and exact analytical result (dashed line) for the $k=0$, "independent" case with radiative decay [Eq. (9)]. The fraction of A [panel (a)] and B [panel (b)] populations is plotted as a function of dimensionless time Dt/d_0^2. The values of $D=0.8$ cm^2/s and $\tau_r=100$ ps were taken from previously reported experimental results (Ref. 8) while d_0 was set to 20 nm ($\nu=0.05$) corresponding to an initial density of 5×10^5 cm^{-1}.

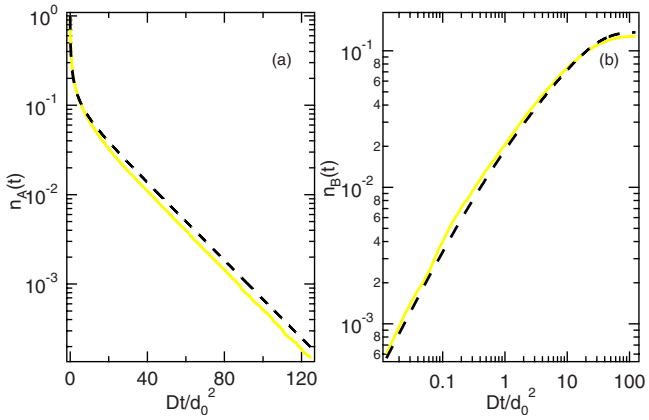

FIG. 2. (Color online) Comparison of Monte Carlo simulations (solid line) and approximate analytical result (dashed line) for $k=0$ "correlated pair" case with radiative decay [Eq. (9)]. (a) The population fraction of A (a) and B (b) as a function of "dimensionless" time. Approximate result agrees fairly well with the simulations. The parameters for simulations are the same as in Fig. 1 except with $d_0=10$ nm ($\nu=0.025$). Some reasons for disagreement with the simulations are discussed in the text.

Figure 1 compares the result of Eq. (9) with Monte Carlo simulations, done by simulating the Brownian diffusive motion of each independent pair of particles, validating our results. As ν is the only physical parameter in the problem, changing d_0 and D but keeping ν constant should not alter the result, which was indeed confirmed by simulations. This fact should remain true even for the case of correlated pairs.

Let us consider the behavior of $n_A(t)$ in the long and short time limits. For $t\gg1$, only the radiative decay should dominate as the density of particle becomes too low to participate in annihilation. Thus, an exponential decay is expected. Taking limits explicitly, one obtains

$$n_A(t\to\infty)=\frac{\exp(-\gamma_r t)}{1+1/\sqrt{\nu}}. \tag{10}$$

As ν is less than unity, so is the intercept of the above exponential decay, hinting at the superexponential decay at short times due to annihilation. In the short time limit, when $\nu<1$ one expects only annihilation to dominate the decay, and one gets

$$n_A(t\to0)=1-2\sqrt{\gamma_r t/\pi\nu}. \tag{11}$$

which is indeed faster than an exponential decay as $t\to0$. Indeed, Fig. 1 confirms these findings. As the time progresses, the density of particles decreases due to decreasing population, which slows down the annihilation reaction as it strongly depends on the density of the particles. The radiative decay rate, on the other hand, is fixed, and thus, a crossover from annihilation dominated decay to a purely exponential radiative decay is expected. It can be defined to take place when $d_t=L/2N_0n_A(t)$ becomes equal to ν. This time τ^* is implicitly given as

$$n_A(\tau^*)=\sqrt{\nu}. \tag{12}$$

As the initial density is increased, τ^* decreases and finally vanishes at very high density, implying a purely exponential decay at all times.

In order to calculate $n_B(t)$, we note that at any given time the rate of radiative decay is proportional to the instantaneous population of A, $n_A(t)$. In other words,

$$\partial_t n_B(t)=\gamma_r n_A(t). \tag{13}$$

Hence, $n_B(t)$ can be obtained from Eq. (9), upon direct integration, as

$$n_B(t)=\gamma_r\int_0^t d\tau n_A(\tau). \tag{14}$$

In particular, the fraction of total population that decays radiatively is given by

$$n_B(\infty)=\frac{1}{1+1/\sqrt{2\nu}}. \tag{15}$$

The study of independent pair model identifies the relevant parameters of the process and the scaling relationships they must obey. It also provides the decay regimes that are relevant for each type of reaction viz., annihilation and radiative decay. The use of purely stochastic first-passage time distribution makes the solution transparent and simple, relying on the properties of diffusion rather than other formal methods, which although more general are less intuitive.

C. Annihilation with decay; $k=0$: Correlated pair case

As for the case of no decay, we scale the mean separation between the particles by a factor of 2 in order to obtain a solution for the correlated case. This approximate solution

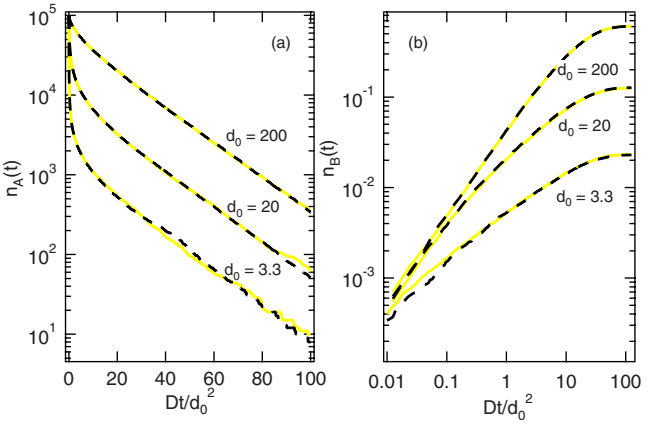

FIG. 3. (Color online) Comparison of $k=1$ (solid line) and $k=0$ (dashed line) for different values of d_0 (in nm) for the "correlated" case with radiative decay. (a) The population fraction of A (a) and B (b) as a function of dimensionless time. d_0 values for $k=1$ case simulations are half of the $k=0$ case shown on the graph). Rest of the parameters are the same as in Fig. 1.

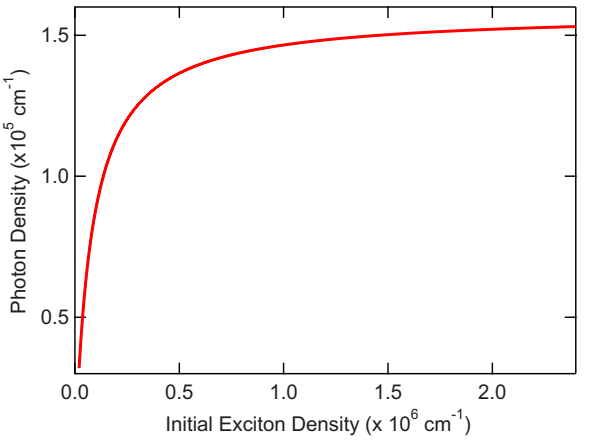

FIG. 4. (Color online) Population per unit length of photons plotted against the initial density of excitons using Eq. (15) to show the saturation behavior in PL intensity predicted by our model. The values of relevant parameters and the range of initial densities are chosen to enable direct comparison with the experimental results of Murakami and Kono (Ref. 4) (see text for details).

and the Monte Carlo simulations for the correlated case are compared in Fig. 2. The approximate solution agrees well with the simulations. A possible reason for the slower decay of analytical result compared to the exact result could be the following: for the single pair case, if one of the particle decays before undergoing collision, the remaining particle *must* decay radiatively and cannot undergo annihilation. However, for the correlated case, this is not true as long as there are other neighboring particles and so annihilation becomes possible.

D. Annihilation with/without decay; $k=1$

The case of partial annihilation [$k=1$ in Eq. (2a)] can be understood in terms of the results for $k=0$. Both processes are completely identical besides the fact that the annihilation in $k=1$ is half as slow as the $k=0$ case. Consequently, if the initial density for the partial annihilation case is twice as much as the complete annihilation case, one expects the two decays to be identical. Thus, the result for the $k=1$ case can be obtained from Eq. (5) by replacing d_0 with $d_0/2$. Even in the presence of radiative decay, the above argument should be true as the radiative decay occurs completely independently of the annihilation reaction. We verify this heuristic reasoning by Monte Carlo simulations, as shown in Fig. 3.

IV. COMPARISON WITH EXPERIMENTAL RESULTS

We use Eq. (15) to calculate the density of species B, or photons created as a function of initial density of species A, or excitons. In terms of experimental parameters, the density of photons created is proportional to the measured PL intensity while the initial density of excitons is proportional to the fluence of the pump laser. A saturation behavior in the PL intensity is seen with increasing density of excitons as shown in Fig. 4.

It is interesting to note that the only physical parameters of importance in our model are D and τ_r, which can be combined to give an "exciton diffusion length" $l_D=\sqrt{D\tau_r}$. In Fig. 4, we chose $l_D=90$ nm so as to quantitatively compare our results with the experimental results of Murakami and Kono,[4] who report a saturation photon density of $\sim 1.7\times 10^5$ cm^{-1} for an initial exciton density of $1-2\times 10^6$ cm^{-1} in a (6,5) nanotube at room temperature. These numbers are in excellent agreement with our model which predicts a saturation photon density of $\sim 1.5\times 10^5$ cm^{-1} at similar initial exciton densities as shown in Fig. 4.

Thus, we see that a new length scale, l_D, arises in the presence of diffusion-driven EEA, which should be compared to other length scales such as d_0 and a_B. When the initial density of created excitons is low, or in other words, d_0 is large compared to l_D, EEA is not very effective and we see a linear increase in PL with increasing exciton density, as shown in Fig. 4. Moreover, as long as the Bohr radius of the excitons, a_B, is much smaller than l_D, it becomes irrelevant in our model. This is indeed the case for the experiments of Murakami and Kono, where $l_D\sim 90$ nm while $a_B\sim 1.5$ nm. As expected from the relative length scales, the Mott density in the above case (7×10^6 cm^{-1}) is about 2 orders of magnitude larger than the saturation density, and hence the Mott density is not sustained due to efficient EEA.

V. DIAMETER, CHIRALITY, AND TEMPERATURE DEPENDENCE

In this section we discuss the dependence of the EEA process on nanotube parameters such as diameter (d_t) and chirality and external parameters such as temperature and magnetic field. As mentioned in Sec. III, the only relevant physical parameters in our model are the diffusion constant D and the radiative lifetime τ_r which enter as the diffusion length l_D, besides the experimentally controllable quantity, d_0. Thus, any dependence of EEA on the parameters of nanotubes such as the diameter and chirality on EEA enters im-

plicitly through the dependence of l_D on them.

The diffusion constant D can be approximated through the Einstein relation,

$$D = \frac{k_B T}{M\Gamma}, \tag{16}$$

where M is the mass of the exciton and Γ is the exciton-phonon scattering rate. For nanotubes, the phonon scattering rate is given in terms of the deformation potential Ξ as[27]

$$\Gamma = \frac{\sqrt{2Mk_BT}\Xi^2 F_{\theta_c}}{\hbar^2 \rho v_L^2}, \tag{17}$$

where ρ is the linear mass density proportional to the diameter d_t, v_L is the longitudinal sound velocity. The chirality dependence is contained in F_{θ_c} as[27]

$$F_{\theta_c} = (1+\nu_P)^2 \cos^2(3\theta_c) + \left(\frac{v_L}{v_T}\sin^2(3\theta_c)\right), \tag{18}$$

where ν_P is Poisson's ratio, θ_c is the chiral angle, and v_T is the transverse sound velocity. Thus,

$$D \propto d_t^{5/2} T^{1/2}, \tag{19}$$

assuming that the exciton mass approximately varies inversely with the diameter.[28]

The radiative lifetime τ_r of excitons in nanotubes exhibits nontrivial dependence on the temperature and diameter due the presence of optically inactive or "dark" excitonic states that are energetically lower than the optically active or "bright" excitonic states.[29,30] This dependence is given as[30,31]

$$\tau_r \propto d_t^3 T \exp\left(\frac{A}{d_t^2 T} - 1\right). \tag{20}$$

Here, A depends on the singlet dark-bright splitting energy and is related to the temperature at which the radiative decay rate attains its maximum.[30]

Combining Eqs. (19) and (20), we get the dependence of l_D as

$$l_D \propto T^{0.75} d_t^{2.75} \exp\left(\frac{A}{2d_t^2 T} - 0.5\right). \tag{21}$$

The effect of the exponential term in Eq. (21) is to cause an increasing trend in l_D below a certain temperature or diameter depending on the value of A, thereby making EEA favorable. In addition, due to the chirality dependence of both D and τ_r,[30] l_D is expected to show alternating behavior arising from the possible values of mod$(n-m,3)$. Thus, the EEA process, which is characterized by l_D, decreases sharply with the diameter of the nanotube until a critical value is reached. Likewise, the EEA process is expected to slow down with decreasing temperature until a transition temperature (T^*), depending on the value of A, is reached. This nonmonotonic behavior of EEA stems from the unique temperature dependence of τ_r of excitons in nanotubes. On the other hand, the τ_r of a *single* 1D exciton band is predicted to scale as[32] $T^{1/2}$, leading to l_D also being proportional to $T^{1/2}$. Hence, EEA would monotonically slow down in such a case.

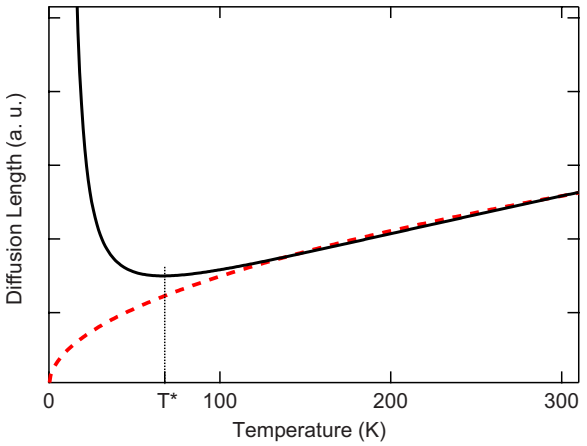

FIG. 5. (Color online) A schematic plot depicting the temperature dependence of exciton diffusion length, l_D, for the case of nanotube with lowest energy excitonic state being optically inactive or "dark" [solid line, Eq. (21)]; and for a single 1D exciton band showing $T^{1/2}$ dependence (dashed line). The value of T^* in the plot is chosen such that it corresponds to a dark-bright splitting $\sim$5.5 meV for a nanotube with $d_t \sim 1$ nm (Ref. 30). It is further assumed that the values of l_D for the two cases are the same at 300 K.

By applying symmetry breaking perturbations such as a magnetic field to the nanotubes, the dark state can be brightened,[33,34] restoring this temperature dependence, and making the attainment of higher excitonic densities possible. Under such conditions, it may be possible to attain the Mott density of excitons in carbon nanotubes. The temperature dependence of l_D for the case of nanotubes with the dark excitonic state lying at a lower energy than the bright exciton is compared with the case of single 1D exciton band in Fig. 5, showing an increasing trend in l_D below T^* for the former case. The value of T^*, as mentioned earlier, is sensitive to the dark-bright splitting. Sustaining high densities of excitons is the first step for any lasing applications and for observing excitonic Bose-Einstein condensation in carbon nanotubes. In addition, at lower temperatures, exciton localization due to impurity traps or defects could completely stop the diffusive motion of excitons,[35] further enabling the attainment of the Mott density.

Finally, in our model, we have assumed a completely random motion of excitons, which leads to ordinary diffusion based on a Gaussian kernel. This assumption can also break down at lower temperatures or in other scenarios when D becomes position or density dependent, leading to anomalous diffusion and changing the time dependence of excitonic population. A time-resolved experiment, probing the excitonic or the photon population at different temperatures, exciton densities, and magnetic fields, cannot only verify the validity of this model but also provide further insight into the EEA process in carbon nanotubes.

VI. SUMMARY

To provide physical insights into the recently observed photoluminescence saturation behaviors in single-walled car-

bon nanotubes, we studied the diffusion and two-particle annihilation of one-dimensional excitons in the general context of reaction-diffusion processes, for which exact treatments exist. By including the radiative recombination decay as a Poissonian process in the exactly solvable problem of one-dimensional diffusion-driven two-particle annihilation, we were able to correctly simulate the density of excitons in single-walled carbon nanotubes as a function of time and density. Monte Carlo simulations were also performed by simulating the purely stochastic, Brownian diffusive motion of one-dimensional excitons, validating our results. Finally, we discussed the diameter, chirality, and temperature dependence of EEA.

ACKNOWLEDGMENTS

We thank the Robert A. Welch Foundation (Grant No. C-1509), NSF (Grants No. DMR-0325474 and No. OISE-0530220), and ARO (Grant No. 49735-PH). One of us (A.S.) would like to thank M. R. Choudhury and Y. Murakami for helpful discussions.

*Corresponding author. Present address: Institute of Quantum Electronics, ETH Hönggerberg, Wolfgang-Pauli Strasse 16, CH-8093 Zürich, Switzerland; sriva@phys.ethz.ch

[1] M. S. Dresselhaus, G. Dresselhaus, R. Saito, and A. Jorio, Annu. Rev. Phys. Chem. **58**, 719 (2007).
[2] Y.-Z. Ma, L. Valkunas, S. L. Dexheimer, S. M. Bachilo, and G. R. Fleming, Phys. Rev. Lett. **94**, 157402 (2005).
[3] G. N. Ostojic, S. Zaric, J. Kono, V. C. Moore, R. H. Hauge, and R. E. Smalley, Phys. Rev. Lett. **94**, 097401 (2005).
[4] Y. Murakami and J. Kono, Phys. Rev. Lett. **102**, 037401 (2009).
[5] N. Mott, *Metal-Insulator Transitions* (Taylor and Francis, London, 1974).
[6] C.-X. Sheng, Z. V. Vardeny, A. B. Dalton, and R. H. Baughman, Phys. Rev. B **71**, 125427 (2005).
[7] R. M. Russo, E. J. Mele, C. L. Kane, I. V. Rubtsov, M. J. Therien, and D. E. Luzzi, Phys. Rev. B **74**, 041405(R) (2006).
[8] L. Cognet, D. A. Tsyboulski, J. R. Rocha, C. D. Donyle, J. M. Tour, and R. B. Weisman, Science **316**, 1465 (2007).
[9] D. Ben-Avraham and S. Havlin, *Diffusion and Reactions in Fractals and Disordered Systems* (Cambridge University Press, Cambridge, 2000).
[10] J. L. Cardy, *The Mathematical Beauty of Physics* (World Scientific, Singapore, 1996).
[11] J. Marro and R. Dickman, *Nonequilibrium Phase Transitions in Lattice Models* (Cambridge University Press, Cambridge, 1999).
[12] G. Odor, Rev. Mod. Phys. **76**, 663 (2004).
[13] A. Okubo, *Diffusion and Ecological Problems: Mathematical Models* (Springer-Verlag, New York, 1980).
[14] H. Hinrichsen, Adv. Phys. **49**, 815 (2000).
[15] A. Kamenev, *Strongly Correlated Fermions and Bosons in Low-Dimensional Disordered Systems* (Kluwer Academic Press, Dordrecht, 2002).
[16] A. Kamenev, *Nanophysics: Coherence and Transport* (Elsevier, Amsterdam, 2005).
[17] G. Polya, Math. Ann. **84**, 149 (1921).
[18] J. Cardy and U. Tauber, J. Stat. Phys. **90**, 1 (1998).
[19] V. Perebeinos, J. Tersoff, and P. Avouris, Phys. Rev. Lett. **94**, 027402 (2005).
[20] D. C. Torney and H. M. McConnell, J. Phys. Chem. **87**, 1941 (1983).
[21] D. Toussaint and F. Wilczek, J. Chem. Phys. **78**, 2642 (1983).
[22] D. ben-Avraham, Phys. Rev. Lett. **81**, 4756 (1998).
[23] J. L. Spouge, Phys. Rev. Lett. **60**, 871 (1988).
[24] A. V. Barzykin and M. Tachiya, Phys. Rev. B **72**, 075425 (2005).
[25] A. V. Barzykin and M. Tachiya, J. Phys. Condens. Matter **19**, 065105 (2007).
[26] I. Karatzas and S. Shreve, *Brownian Motion and Stochastic Calculus* (Springer, New York, 2004).
[27] G. Pennington and N. Goldsman, Phys. Rev. B **71**, 205318 (2005).
[28] T. Ando, J. Phys. Soc. Jpn. **73**, 3351 (2004).
[29] C. D. Spataru, S. Ismail-Beigi, R. B. Capaz, and S. G. Louie, Phys. Rev. Lett. **95**, 247402 (2005).
[30] V. Perebeinos, J. Tersoff, and P. Avouris, Nano Lett. **5**, 2495 (2005).
[31] R. B. Capaz, C. D. Spataru, S. Ismail-Beigi, and S. G. Louie, Phys. Rev. B **74**, 121401(R) (2006).
[32] D. S. Citrin, Phys. Rev. Lett. **69**, 3393 (1992).
[33] J. Shaver, J. Kono, O. Portugall, V. Krstic, G. L. J. A. Rikken, Y. Miyauchi, S. Maruyama, and V. Perebeinos, Nano Lett. **7**, 1851 (2007).
[34] A. Srivastava, H. Htoon, V. I. Klimov, and J. Kono, Phys. Rev. Lett. **101**, 087402 (2008).
[35] A. Hogele, C. Galland, M. Winger, and A. Imamoglu, Phys. Rev. Lett. **100**, 217401 (2008).